

ON THE ANALYSIS AND DESIGN OF REINFORCED CONCRETE BEAMS STRENGTHENED WITH FRP LAMINATES

A. M. Malek

*Department of Civil Engineering
Lamar University
Beaumont, Texas, 77710, U.S.A.*

and H. Saadatmanesh*

*Department of Civil Engineering and Engineering Mechanics
University of Arizona
Tucson, AZ, 85721, U.S.A.*

الخلاصة :

من الممكن زيادة قوة الثني والقص بفعالية لكمرات الخرسانة المسلحة عن طريق إصاق لوح لسطح الشد أو وتر الكمرة. ويتعرض اللوح بذلك إلى جهود شدّ وبذلك يقاوم حدوث التصدعات في الخرسانة. في هذه الورقة تمّت مراجعة دراسة معملية وتحليلية لكمرات خرسانية تمّت تقويتها عن طريق إصاق لوح من البلاستيك المعرّز بالألياف للكمرات الخرسانية باستخدام مادة الأيبوكسي اللاصقة. كما تمّ تقديم دليل إرشادي ومعادلات لتقوية مقاومة الثني لكمرات الخرسانة. كما تمّ استعراض أشكال مختلفة من الإنهيارات مثل تفتت الخرسانة بفعل الانضغاط وتمزق اللوح أو النسيج، والانهيال بفعل القصّ الموضعي، وذلك لتطوير الدليل الإرشادي. كما نُوقش تأثير إصاق اللوح المركّب أو النسيج بوتر الكمرة الخرسانية على مقاومة وقوة القص.

ABSTRACT

Flexural and shear strength of reinforced concrete beams can be effectively increased by bonding a composite plate to the tension face or web of the beam. The plate undergoes tensile stresses and resists opening of the cracks. In this paper, experimental and analytical study of concrete beams strengthened with epoxy bonded fiber composite plate or fabric is reviewed. Guidelines and equations are also presented for flexural strengthening of concrete beams. Different modes of failure such as compression crushing of concrete, rupture of the plate and local shear failure have been considered in the development of the guidelines. The effect of web-bonded composite plate on the shear strength of the concrete beam is also discussed.

*To whom correspondence should be addressed.

ON THE ANALYSIS AND DESIGN OF REINFORCED CONCRETE BEAMS STRENGTHENED WITH FRP LAMINATES

INTRODUCTION

Epoxy bonding a plate to the tension face or web is an effective technique for flexural or shear strengthening of reinforced concrete beams (Figure 1). The effect of steel plates when bonded to the tension face has been studied extensively [1–5]. The main drawback in this strengthening system is the corrosion of steel plate, which adversely affects the bond between the plate and the concrete. The problem is more severe for bridges where deicing chemicals are normally used during cold seasons. In order to eliminate the corrosion problem, steel plates have been replaced by corrosion-resistant fiber reinforced plastic (FRP) plates or laminates. Besides corrosion resistance, other advantages such as formability and high strength and light weight have made FRP a desirable substitute for conventional materials. Fiber composites are made from high-strength filaments of glass, carbon, or kevlar placed in a resin matrix. The fibers provide the main structural characteristics of the composite. The resin provides shear transfer between the fibers as well as protects the fibers from abrasion and other mechanical and environmental factors. Depending on the design requirements and cost, composites can be produced from a variety of different fibers and resins [6].

Some of the early experiments on reinforced concrete beams strengthened with FRP plates carried out in 1991 [7, 8], revealed an appreciable improvement in the strength of the beam as a result of bonding the composite plate. In a subsequent analytical study based on compatibility of strains in the cross section of the strengthened beam, the load–deflection diagram was generated and compared to that of unretrofitted beam as shown in Figure 2 [9, 10]. It can be seen that the strength of the beam was increased several fold as a result of bonding the plate. There was a good agreement between the experimental results and the predicted ones. However, local shear failure between the plate and the beam, a commonly observed mode of failure as shown in Figure 3, could not be predicted without consideration being given to the stress concentration at the plate cut-off points as well as at the flexural crack tips. In a recent study, closed form solutions were developed that predict the shear and normal stress concentrations at the plate cut-off point. Design guidelines and equations were also developed to provide the necessary design tools for practicing engineers involved in retrofit and repair projects [11–13].

Fiber composite plates or laminates can also be bonded to the web of concrete beams to increase the shear capacity of the beam. This type of shear strengthening has been investigated both experimentally and analytically [11, 14–16]. Local debonding of the plate due to shear stress concentration at the location of the cracks is still under investigation, but effectiveness of this method has been confirmed by theoretical and experimental results.

This paper presents a comprehensive summary of the analysis and design procedures for concrete beams externally strengthened by FRP laminates.

FLEXURAL ANALYSIS

Bonding a composite laminate to tension flange will effectively increase the flexural capacity of reinforced concrete beams. This increase is the result of an internal moment consisting of the tensile force in the plate and an equivalent compressive force in the concrete. In an experimental study of the behavior of the strengthened beams, five rectangular reinforced concrete beams and a T-beam were strengthened by epoxy bonded glass fiber reinforced plastic (GFRP) plates and loaded to failure [7]. Different modes of failure including crushing of concrete in compression, debonding of the composite plate, and sudden failure of concrete layer between the plate and longitudinal steel rebars were observed. The

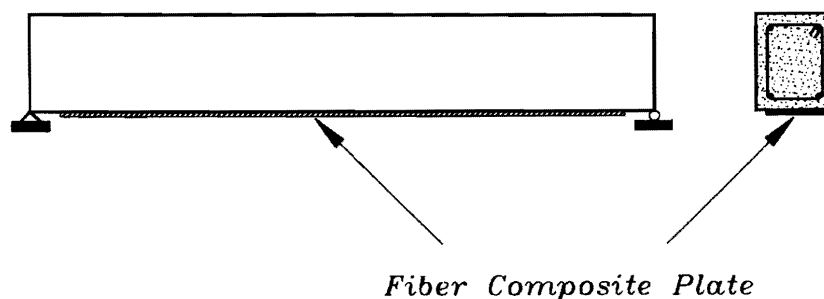


Figure 1. Flexural Strengthening of Reinforced Concrete Beams with Composite Laminates.

latter failure mode which has also been observed by other researchers [8] is referred to as “local failure” and it results from shear and normal (peeling) stress concentrations at the plate end. The results of this study, however, indicated that significant increase in the flexural strength is achieved by bonding the GFRP plate to the tension face, regardless of the mode of failure. This method of strengthening is more effective for beams with lower steel reinforcement ratio. The size of the cracks and displacement at failure of the beam were reduced as a result of bonding the plate. The local shear failure was pointed out as an important mode of failure in the strengthened beam, which may prevent the beam from reaching its full flexural capacity. Based on variations of strains across the depth of the cross section of the strengthened beam, analytical models were

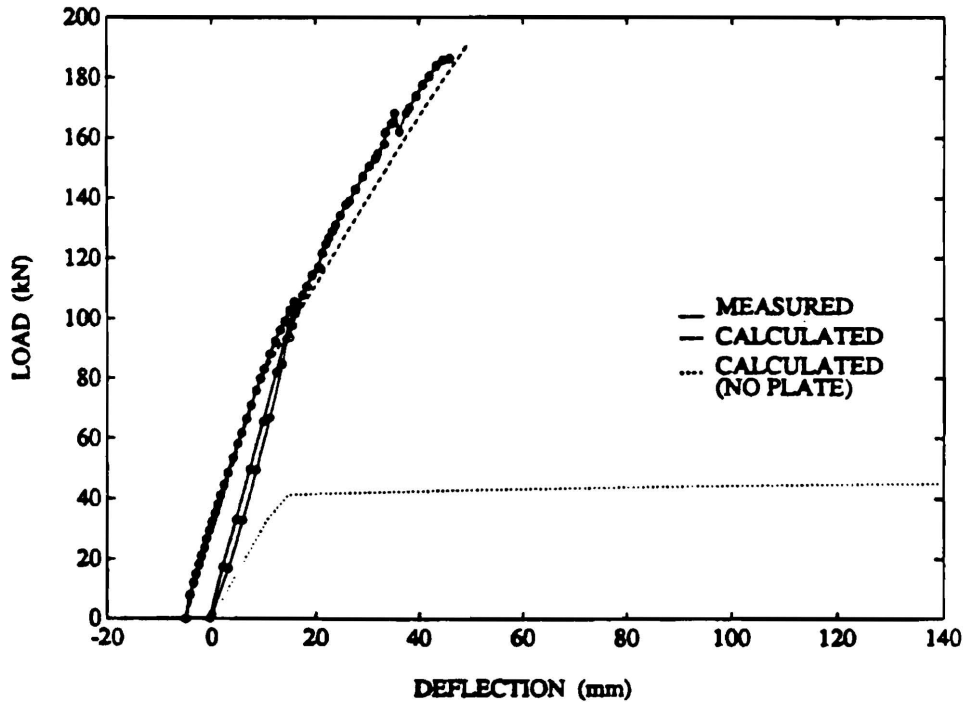


Figure 2. Load-Deflection Diagram of the Beam Before and After Strengthening [9].



Figure 3. Local Shear Failure in Strengthened Beam.

developed to predict the stresses and deformations of rectangular and T-beams [10]. Moment–curvature diagrams were generated for both rectangular and T-cross sections. Effects of several design parameters such as the cross sectional area of steel reinforcement and composite plate, ultimate strength of the plate, and compressive strength of concrete were investigated through a parametric study. In spite of the good prediction of the moment–curvature diagram, the models were limited to failure by either crushing of concrete or rupture of the plates. The model was unable to predict the failure due to debonding of the plate around the flexural cracks or local shear failure at the plate end.

Analysis for Stress Concentrations

In order to predict the shear and normal stress concentrations at the plate end, an analytical model was developed and its results were compared to the finite element analysis [11, 12]. The main assumptions in developing the model were linear elastic behavior of the materials, no slip and uncracked section. In this model, the shear stress in the adhesive layer, $\tau(x)$, was related to the normal stress in the plate, $f_p(x)$, through using the following simple relationship:

$$\tau(x) = \frac{df_p(x)}{dx} t_p \tag{1}$$

where t_p is the thickness of the plate. By relating the shear stress to the longitudinal displacements at the top and bottom faces of the adhesive, the governing differential equation for the axial stress in the plate can be developed [11, 12]. Solving the differential equation and applying appropriate boundary conditions, the following equation for the maximum shear stress in the adhesive layer at the cut-off point is obtained:

$$\tau_{\max} = t_p (b_3 \sqrt{A} + b_2) . \tag{2}$$

In the above equation: $A = \frac{G_a}{t_a t_p E_p}$, $b_1 = \frac{\bar{y} a_1 E_p}{I_r E_c}$, $b_2 = \frac{\bar{y} E_p}{I_r E_c} (2a_1 L_o + a_2)$, and

$$b_3 = E_p \left[\frac{\bar{y}}{I_r E_c} (a_1 L_o^2 + a_2 L_o + a_3) + 2b_1 \frac{t_a t_p}{G_a} \right]$$

where: a_1 , a_2 , and a_3 are obtained from the bending moment equation for distributed load as shown in the following:

$$M(x_o) = a_1 x_o^2 + a_2 x_o + a_3 .$$

Furthermore, G_a , t_a = shear modulus and thickness of adhesive, respectively, E_p and E_c = modulus of elasticity of composite plate and concrete, respectively, L_o = distance between the cut-off point and the support of the beam, \bar{y} = distance from neutral axis of the strengthened section to the center of the FRP Laminate, and I_r = moment of inertia of the transformed section based on concrete.

Figure 4 shows the variations of the shear stresses along the beam based on the analytical model presented above and the finite element analysis, for three different meshes.

The associated maximum normal (peeling) stress at the cut-off point is obtained as [11, 12]:

$$f_{n_{\max}} = \frac{k_n}{2\beta^3} \left(\frac{V_p}{E_p I_p} - \frac{V_c + \beta M_o}{E_c I_c} \right) + \frac{q E_p I_p}{b_p E_c I_c} . \tag{3}$$

where: $k_n = \frac{E_a}{t_a}$, $\beta = \left(\frac{k_n b_p}{4 E_p I_p} \right)^{0.25}$, b_p = width of the plate, I_p and I_c = moments of inertia of plate and concrete beam,

q = distributed load acting on the beam, and M_o = bending moment in the concrete beam at the plate-end due to the externally applied loads. The shear forces caused by shear stress concentration in the plate and concrete beam, V_p and V_c are calculated from the following equations:

$$V_p = -\frac{1}{2} b_p t_p^2 (b_3 \sqrt{A} + b_2)$$

$$V_c = V_o - b_p \bar{y}_c t_p (b_3 \sqrt{A} + b_2)$$

where V_o is the shear force in the beam at the plate end due to external loads.

Figure 5 shows the variations of the normal stresses along the beam from the results of the analytical model presented here and the finite element analysis for the beam shown in Figure 4. The bending stress in the concrete beam at the cut-off point of the plate is increased as a result of shear stress concentration. This increase is obtained from the following equation and is discussed in details in [11, 12]:

$$M_m = L_o t_p b_p \bar{y}_c (b_3 \sqrt{A} + b_2) \tag{4}$$

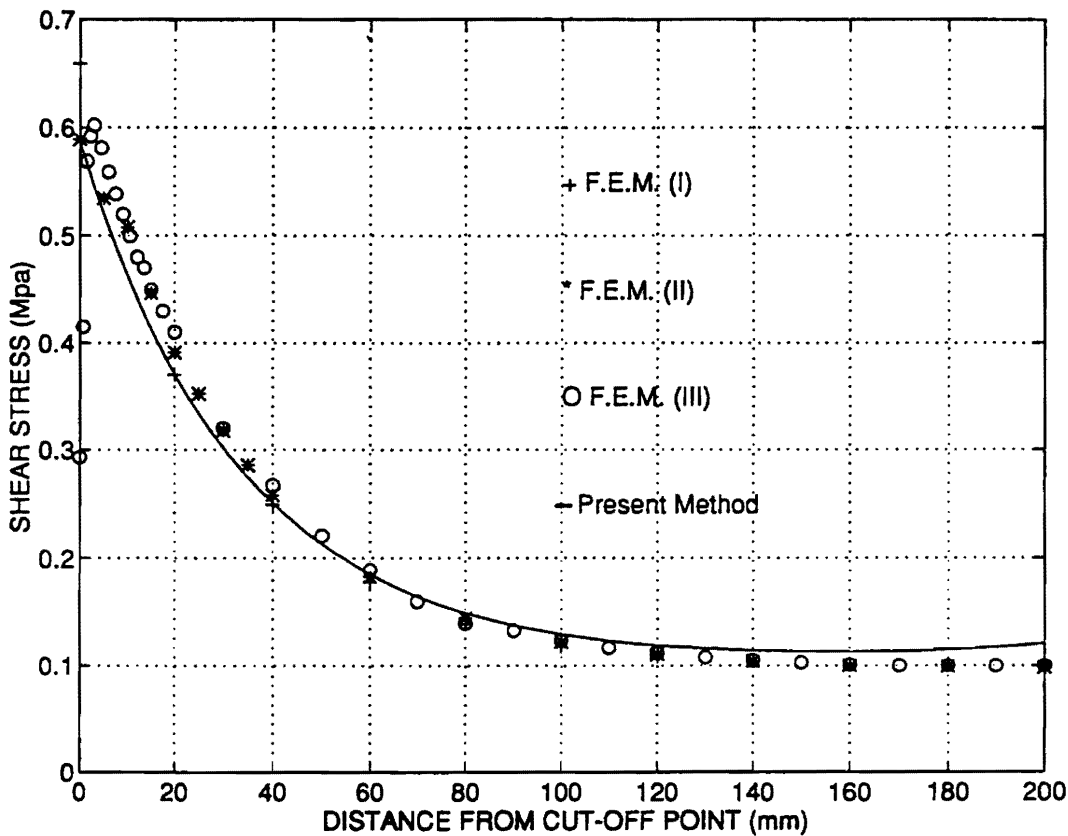
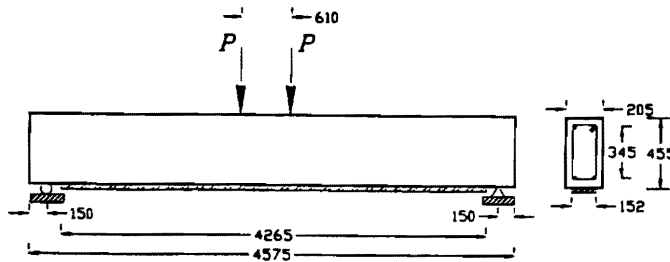


Figure 4. Comparison of Analytical Model to Finite Element Analysis (Shear Stress).

where: \bar{y}_c = distance between the neutral axis and the tension face of concrete beam. This moment is added to the bending moment at the cut-off point due to external loads to calculate the flexural stresses.

The results of the analytical model were also compared to the available experimental results. There was a good agreement between the results of the analytical model and the experimental data [11, 12].

SHEAR ANALYSIS

Shear strength of concrete beams can be increased by bonding the composite laminates to the web, or wrapping composite fabric in the form of a U-shape around the beam as shown in Figure 6. A series of twenty-one beams were tested to reveal the effectiveness of this technique [14]. Carbon sheets were bonded by epoxy resins to two types of short and long beam specimens. The short beams were used as shear specimens, and the long ones as flexural. Three different types of FRP systems with four different fiber orientations were used. Some of the beams were strengthened over the entire length, while others were strengthened only near the supports (Figure 6). In order to simulate the effect of the initial cracking of the beam prior to bonding the plate, several beams were precracked before strengthening.

The effect of web-bonded plates was not significant before yielding of the steel rebars. Thereafter, the effect of the plate was appreciably increased as a result of its resistance against opening of the cracks. Depending on fiber orientation, different modes of failure were observed. Beams strengthened with $[0/90^\circ]$ fibers experienced crushing of concrete, rupture of the plate or failure of concrete layer between the composite plate and the longitudinal steel reinforcement. For concrete beams strengthened with laminates of $[45/-45^\circ]$ fiber orientations, the increase in the flexural capacity was lower, and they failed in a ductile manner. In all the cases, the bonded composite had a significant effect on the ultimate flexural or shear strength of the beam [14].

The effect of the plate (fabric) on the shear strength of concrete beams has been analytically studied before and after formation of shear cracks. The shear force resisted by the plate or fabric prior to formation of shear or flexural cracks is not appreciable and can be neglected. In investigating this effect, a parametric study was carried out. Based on linear elastic

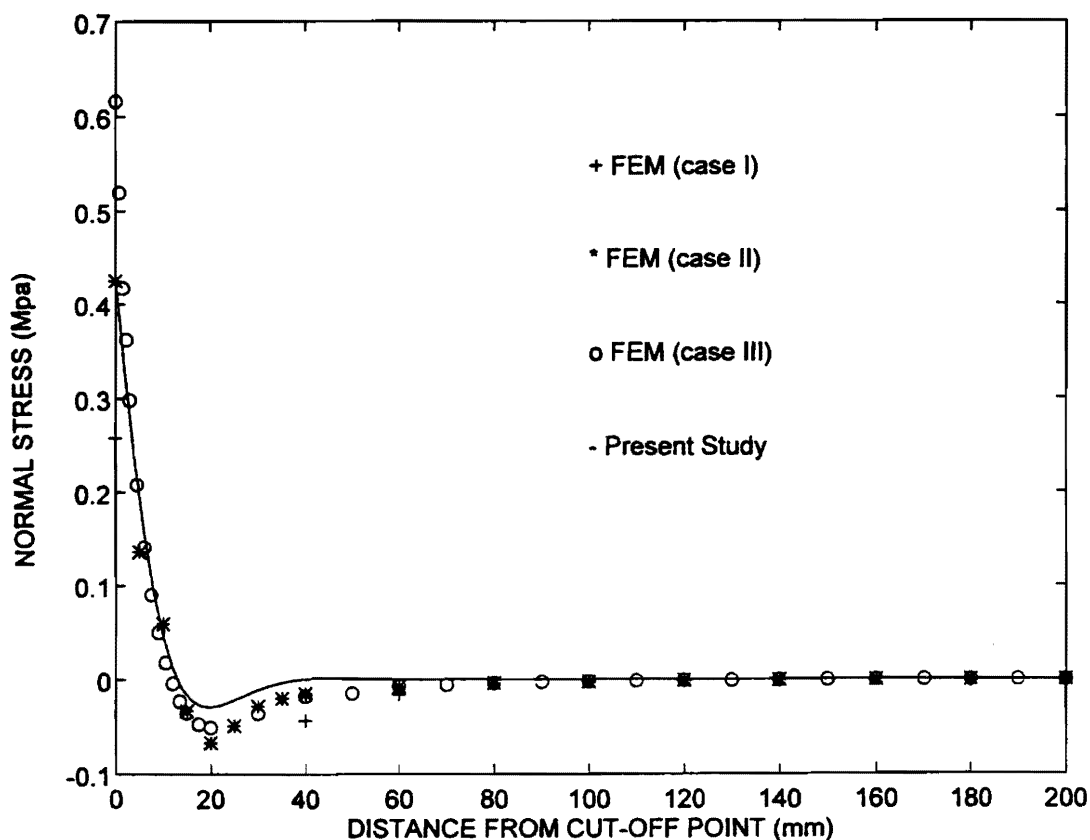


Figure 5. Comparison of Analytical Model to Finite Element Analysis (Normal Stress).

behavior of the material, and complete bonding between the plate and the beam, equations were developed for both uncracked beam and beam with flexural cracks [11, 15]. The effects of different parameters such as fiber orientation, height of the composite plate, and the thickness of the plate were studied for each case. The shear force in the plate is composed of two different components: the first component is caused by orthotropic behavior of the plate, and it is present even if the beam is under pure bending; the second component is caused by variation of bending moment along the beam and is present only if shear force is present. The shear force resisted by the plate is negligible for uncracked beams. However, for cracked beams, the resistance contributed by the composite plate (fabric) is appreciably higher and several parameters such as thickness of the plate and fiber orientation can significantly affect it.

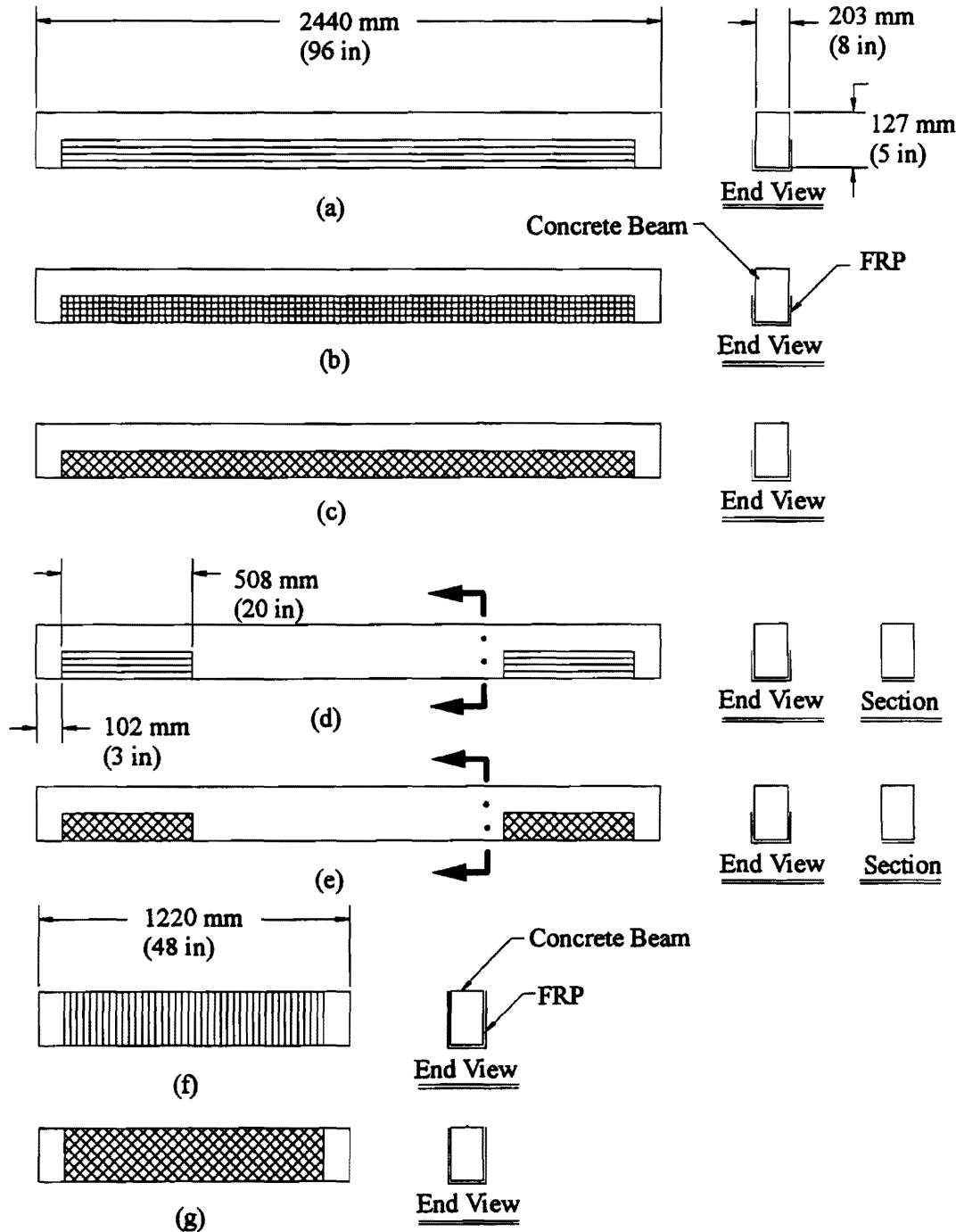


Figure 6. Shear Strengthening of Reinforced Concrete Beams with Composite Laminates [14].

In a later study, the ultimate shear capacity of the beam was the main objective [16]. Truss analogy and compression field theory were utilized in a manner similar to that for ordinary reinforced concrete beams for prediction of the ultimate shear capacity. According to the compression field theory, after formation of inclined shear cracks, concrete does not carry any tensile stress and it acts as a series of compression struts with the same inclination of principle compressive strain. The inclination of the cracks depends on several parameters such as the geometry and material properties of the concrete beam and FRP laminate. Assuming linear elastic behavior for the composite plate, elastic perfectly plastic behavior for steel reinforcement, and ignoring the stress concentration and debonding effects, equations were developed to calculate the axial strain in the concrete compression struts and the longitudinal reinforcement. Using the strain transformation equations, the axial strain in the vertical direction and in the direction perpendicular to struts were calculated and used to obtain the shear force resisted by the strengthened beam. A computer program was developed to carry out the calculations iteratively, and to obtain the correct inclination angle that satisfied both equilibrium and compatibility. Effects of several parameters such as plate thickness, fiber orientation angle, and stirrup spacing on the crack inclination angle were studied. The effect of fiber orientation angle on the crack inclination angle and the ratio of the shear force resisted by the composite plate to the total shear force (F_p/V) are shown in Figure 7.

The analytical models developed in this study can be used to calculate the crack inclination angle. Knowing this angle and assuming that steel stirrups will yield at the ultimate state, and ignoring the shear force resisted by concrete, the following conservative equation is developed to determine the ultimate shear strength of the strengthened beam [11, 16]:

$$V_n = \frac{h_v}{S \tan \theta_c} F_y A_v + \frac{h}{\tan \theta_c} \sigma_n t_p \tag{5}$$

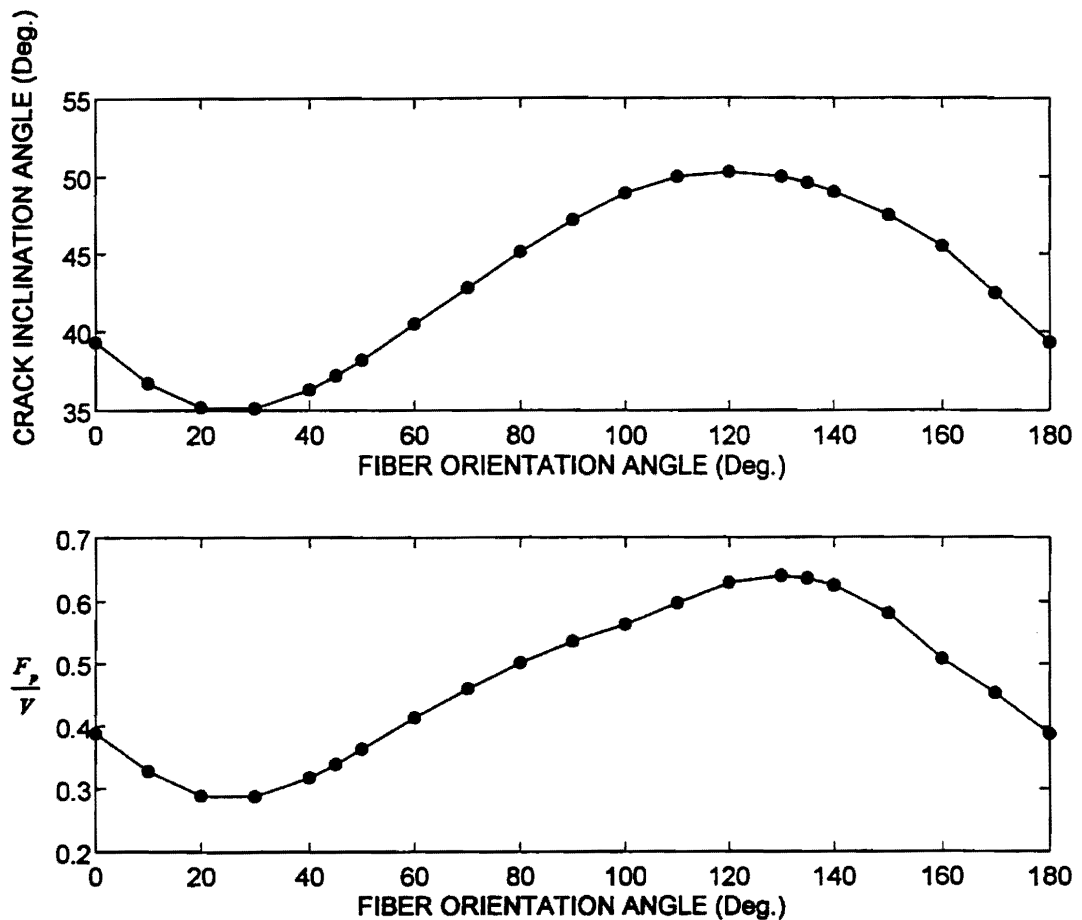


Figure 7. Effect of Fiber Orientation Angle on:
 (a) crack inclination angle;
 (b) the ratio of the shear force resisted by composite plate to total shear force.

where: V_c = shear force resisted by concrete, A_v = cross sectional area of two legs of steel stirrup, S = spacing of stirrups, F_y = yield stress of steel, h_v = depth of concrete enclosed by steel stirrups, t_p = total thickness of composite laminate bonded to both faces of the web, σ_n = ultimate strength of composite plate in the direction normal to crack, and θ_c = crack inclination angle with respect to horizontal axis. A reasonably close agreement was observed between the results of this method and the experimental data.

DESIGN GUIDELINES FOR FLEXURAL STRENGTHENING

In flexural strengthening of concrete beams, the following modes of failure have been reported: compression crushing of concrete, rupture of the composite plate, and local failure in the concrete layer between the plate and the longitudinal tension reinforcement [7, 8]. These modes of failure have been considered in the development of design guidelines that follow.

The following equations and guidelines have been developed in a manner to assure ductility by allowing the tension steel reinforcement to yield before the composite plate ruptures, or concrete crushes in compression.

The plate reinforcement ratio is defined as: $\rho_p = \frac{A_p}{bd}$, where A_p is the area of the plate, b is the width of the reinforced concrete beam, and d is the effective depth of the tension steel rebars (Figure 8). The plate reinforcement ratio is limited to the following maximum value to avoid over-reinforcing of the concrete beam: $\rho_{p,max} = 0.75 \rho_{p,b}$. (The reduction factor 0.75 used here is similar to that for reinforced concrete beams due to the lack of studies to accurately define this factor.) Additional studies need to be conducted to determine an appropriate reduction factor for this type of reinforcement.

In the above expression, $\rho_{p,b}$ is calculated using one of the following equations:

- If compression steel has yielded:

$$\rho_{p,b} = \frac{\rho'f_y + 0.85f'_c\beta_1\eta_1 - \rho f_y}{\left(\epsilon_u \frac{h - \eta_1 d}{\eta_1 d} - \epsilon_{po}\right)E_p} \quad (6)$$

- If compression steel has not yielded:

$$\rho_{p,b} = \frac{\left(\frac{\eta_1 d - d'}{\eta_1 d}\right)E_s\rho' + 0.85f'_c\beta_1\eta_1 - \rho f_y}{\left(\epsilon_u \frac{h - \eta_1 d}{\eta_1 d} - \epsilon_{po}\right)E_p} \quad (7)$$

$$\text{where: } \eta_1 = \frac{\epsilon_u}{\epsilon_u + \epsilon_y} \quad ,$$

ϵ_u = ultimate compression strain of concrete, and ϵ_y = yield strain of steel reinforcement. ρ and ρ' = tension and compression steel reinforcement ratios, respectively, f'_c = compressive strength of concrete, d' = depth of compression steel rebars, h = overall depth of concrete beam, β_1 = parameter of rectangular stress block in concrete as defined in the ACI Code, and f_y = yield stress of steel. The initial strain, ϵ_{po} , will be defined in the subsequent section. In choosing one of the above equations, it is necessary to verify whether the compression steel has yielded or not at the balanced condition. The compression steel yields provided that:

$$d' \leq \left(\frac{\epsilon_u - \epsilon_y}{\epsilon_u + \epsilon_y}\right)d \quad (8)$$

Effect of Initial Strains

For repair and retrofit problems, the effect of strains and stresses that the concrete beam has undergone before bonding the plate must be considered. This effect is taken into account by reducing the axial stress in the composite plate according to the following equation and assuming a linear strain diagram across the depth of the cross section:

$$f_p = E_p(\epsilon_p - \epsilon_{po}), \tag{9}$$

where: f_p = stress in composite plate, E_p = modulus of elasticity of plate in longitudinal direction, ϵ_p = strain in composite plate, ϵ_{po} = initial strain of tension face of beam, before plate bonding. This strain is calculated based on elastic analysis of the section under service loads.

Ultimate Flexural Capacity of Strengthened Beam

The ultimate flexural capacity depends on the governing mode of failure, and also yielding of the compression steel at the ultimate state. Based on the magnitude of the plate reinforcement ratio, ρ_p , one of the following equations may be applied [11, 13].

- (a) If $\rho_{p,cy} \leq \rho_p \leq \rho_{p,bb}$, the mode of failure is due to rupture of the plate, and the compression steel yields at the ultimate state. The nominal flexural capacity is obtained from:

$$M_n = A'_s f_y \left(\frac{\beta_1 c}{2} - d' \right) + A_s f_y \left(d - \frac{\beta_1 c}{2} \right) + A_p f_{pr} \left(h - \frac{\beta_1 c}{2} \right) \tag{10}$$

where: $c = \frac{A_s f_y + A_p f_{pr} - A'_s f_y}{0.85 f'_c b \beta_1}$,

A_s and A'_s = cross sectional area of tension and compression reinforcement, f_{pr} = composite plate stress at rupture, $\rho_{p,bb}$ = balanced plate reinforcement ratio at ultimate state, defined in subsequent sections, and $\rho_{p,cy}$ = plate reinforcement ratio indicating yielding of compression rebars at ultimate state, as defined in subsequent sections.

- (b) If $\rho_p \leq$ smaller of $\rho_{p,bb}$ and $\rho_{p,cy}$, then rupture of the plate is the mode of failure, and compression steel does not yield at the ultimate state. The nominal flexural capacity is obtained from:

$$M_n = \left(\frac{c - d'}{h - c} \right) (\epsilon_r + \epsilon_{po}) A'_s E_s \left(\frac{\beta_1 c}{2} - d' \right) + A_s f_y \left(d - \frac{\beta_1 c}{2} \right) + A_p f_{pr} \left(h - \frac{\beta_1 c}{2} \right) \tag{11}$$

where $\epsilon_r = \frac{f_{pr}}{E_p}$, and the depth of the neutral axis, c , is calculated from the following quadratic equation:

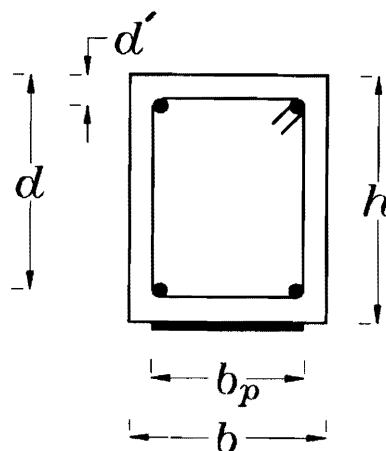


Figure 8. Cross Section of the Strengthened Beam.

$$\bar{A}c^2 + \bar{B}c + \bar{C} = 0 \tag{12}$$

where: $\bar{A} = 0.85f'_c\beta_1b$

$$\bar{B} = -0.85f'_c\beta_1hb - (\epsilon_r + \epsilon_{po})A'_sE_s - A_s f_y - A_p f_{pr}$$

$$\bar{C} = (\epsilon_r + \epsilon_{po})E_s A'_s d' + (A_s f_y + A_p f_{pr})h .$$

(c) If $\rho_{p,bb} \geq$ larger of $\rho_{p,bb}$ and $\rho_{p,cy}$ then crushing of concrete in compression is the mode of failure, and the compression steel yields at the ultimate state. The nominal flexural capacity is obtained from:

$$M_n = A'_s f_y \left(\frac{\beta_1 c}{2} - d \right) + A_s f_y \left(d - \frac{\beta_1 c}{2} \right) + \left(\frac{h-c}{c} \epsilon_u - \epsilon_{po} \right) E_p A_p \left(h - \frac{\beta_1 c}{2} \right) \tag{13}$$

where the depth of the neutral axis, c , is calculated from the following quadratic equation:

$$\bar{A}c^2 + \bar{B}c + \bar{C} = 0 \tag{14}$$

where: $\bar{A} = 0.85f'_c\beta_1b$

$$\bar{B} = (A'_s - A_s) f_y + (\epsilon_u + \epsilon_{po}) E_p A_p$$

$$\bar{C} = -\epsilon_u h A_p E_p .$$

(d) If $\rho_{p,bb} \leq \rho_p \leq \rho_{p,cy}$, then compression crushing of concrete is the mode of failure, and compression steel does not yield at the ultimate state. The nominal flexural capacity is obtained as:

$$M_n = \left(\epsilon_u \frac{c-d'}{c} \right) A'_s E'_s \left(\frac{\beta_1 c}{2} - d' \right) + A_s f_y \left(d - \frac{\beta_1 c}{2} \right) + \left(\frac{h-c}{c} \epsilon_u - \epsilon_{po} \right) E_p A_p \left(h - \frac{\beta_1 c}{2} \right) \tag{15}$$

where the depth of the neutral axis, c , is calculated from the following quadratic equation:

$$\bar{A}c^2 + \bar{B}c + \bar{C} = 0 \tag{16}$$

where: $\bar{A} = 0.85f'_c\beta_1b$

$$\bar{B} = E_s \epsilon_u A'_s - A_s f_y + (\epsilon_u + \epsilon_{po}) E_p A_p$$

$$\bar{C} = -\epsilon_u h A_p E_p - \epsilon_u d' A'_s E_s .$$

In the above cases, $\rho_{p,bb}$, and $\rho_{p,cy}$, are calculated as follows. The balanced plate reinforcement ratio at ultimate state, $\rho_{p,bb}$, is calculated from:

$$\rho_{p,bb} = \frac{0.85f'_c\beta_1 \frac{\eta_3 h}{d} + \rho' \epsilon'_s E_s - \rho f_y}{f_{pr}} \tag{17}$$

where: $\eta_3 = \frac{\epsilon_u}{\epsilon_u + \epsilon_r + \epsilon_y}$

and: $\epsilon'_s = \left(1 - \frac{d'}{\eta_3 h} \right) \epsilon_u \leq \epsilon_y .$

The plate reinforcement ratio, indicating yielding of the compression rebars at the ultimate state, $\rho_{p,cy}$, is obtained from one of the following equations.

- If the rupture of the plate is the governing mode of failure [cases (a) and (b)]:

$$\rho_{p,cy} = \frac{0.85f'_c\beta_1 \frac{c}{d} + \rho'f_y - \rho f_y}{f_{pr}} \quad (18)$$

where: $c = \frac{\epsilon_y h + \epsilon_r d'}{\epsilon_r + \epsilon_y}$.

- If the compression crushing of concrete is the governing mode of failure [cases (c) and (d)]:

$$\rho_{p,cy} = \frac{0.85f'_c\beta_1\eta_2 \frac{d'}{d} + (\rho' - \rho)f_y}{E_p(\epsilon_p - \epsilon_{po})} \quad (19)$$

where: $\eta_2 = \frac{\epsilon_u}{\epsilon_u - \epsilon_y}$, and $\epsilon_p = \epsilon_u \frac{h - \eta_2 d'}{\eta_2 d'}$.

The ultimate flexural capacity of the strengthened beam is then compared to the moment caused by the externally applied loads, considering the load and resistance factors as specified for ordinary reinforced concrete, to verify the adequacy of the design [8, 10].

Local Shear Failure at the Cut-Off Point

Based on the analytical model discussed earlier, the following equations have been obtained for a strengthened beam under uniformly distributed load to predict the maximum shear and normal stresses at the cut-off point [13]:

$$\tau_{max} = \tau_o(1 + \gamma) \quad (20)$$

$$f_{n,max} = \frac{k_n q L}{4\beta^3} \left(\frac{\alpha t_p (1 + \gamma)}{E_p I_p} - \frac{1 - \frac{\alpha h}{2} (1 + \gamma) + \beta L_o}{E_c I_c} \right) \quad (21)$$

where: L = length of the beam, $\tau_o = \frac{t_p E_p \bar{y} L q}{2 I_r E_c}$, $\gamma = L_o \sqrt{\frac{G_a}{t_a t_p E_p}}$, and $\alpha = \frac{b_p t_p E_p \bar{y}}{I_r E_c}$.

Equations 20 and 21, for the special case of uniformly distributed load, were derived from the generalized equations previously defined (Equations (2) and (3)).

The increase in the bending moment at the cut-off point under uniform load is given by [11, 13]:

$$M_m = \frac{\alpha L_o h L q}{4} (1 + \gamma) \quad (22)$$

Failure Criterion

The concrete element located at the cut-off point in the concrete beam, as shown in Figure 9, is under the following state of stresses: σ_x = stress due to bending including the increase in moment, σ_y = peeling (normal) stress at the cut-off point ($f_{n,max}$), τ_{xy} = shear stress at the cut-off point (τ_{max}).

The principal stresses are obtained using stress transformation equations. The maximum principal (tensile) stress is compared to the tensile strength of concrete under biaxial state of stress given in Equation 23 to check the failure.

According to the failure model proposed by Kupfer and Grestle [16], the strength of concrete under tension–tension biaxial state of stress is approximated by:

$$f_{tu} = 0.295(f_{cu})^{2/3} \tag{23}$$

where f_{cu} and f_{tu} (MPa) are the ultimate compressive and tensile strength of concrete, respectively.

Design Example (Flexural Strengthening)

The reinforced concrete beam shown in Figure 10 was originally designed for the following loads:

$$DL = 40 \text{ kN/m}$$

$$LL = 75 \text{ kN/m}$$

The requirement is to increase the flexural live load capacity by 60% to: $LL = 120 \text{ kN/m}$.

The service bending moment and the factored moment at the midspan of the beam before bonding the plate are calculated as: $M_D = 180 \text{ kN-m}$, $M_L = 337.5 \text{ kN-m}$, $M_u = 1.4 M_D + 1.7 M_L = 826 \text{ kN-m}$.

The nominal flexural capacity of the concrete beam is calculated as: $\phi M_n = 847 \text{ kN-m}$.

The factored moment at the midspan of the beam after applying the additional live load is: $M_u = 1170 \text{ kN-m}$. This moment is higher than the capacity of the beam, indicating the need for strengthening. The mechanical properties of the materials are given in Table 1.

Using an elastic analysis for cracked section of the reinforced concrete beam (before upgrading) the location of the neutral axis and the moment of inertia are calculated:

$$\bar{y} = 373 \text{ mm}, I_{tr} = 5.45 \times 10^9 \text{ mm}^4 .$$

Using service load moments ($M_D + M_L$) the initial strain at the tension face of concrete beam is calculated as:

$$\epsilon_{po} = \frac{(M_D + M_L)\bar{y}}{I_{tr}E_c} = 1.27 \times 10^{-3} .$$

Table 1. Mechanical Properties of Materials.

Material Property	Steel (MPa)	Concrete (MPa)	FRP (MPa)	Adhesive (MPa)
E	200 000	27 900	37 230	2 060
f_y	470	—	—	—
f'_c	—	35	—	—
f_u	—	—	390	36
G	—	—	—	751

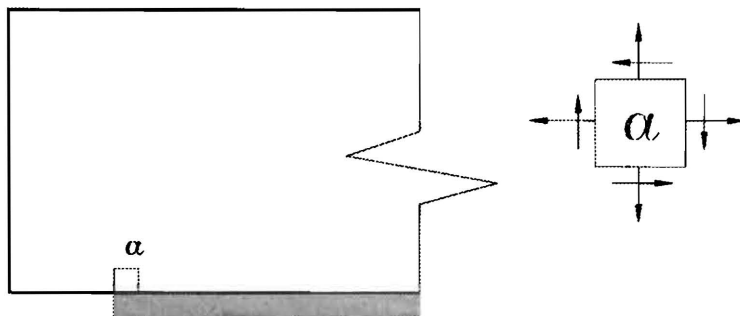


Figure 9. State of Stresses in Concrete Beam at the Cut-off Point.

Assuming $\epsilon_u = 0.003$, and $\epsilon_y = 0.002$, and using Equation 8, it can be concluded that at balanced condition the compression reinforcement has yielded. Using Equation 17, $\rho_{p,bb}$ is obtained as a negative number indicating that crushing of concrete is the predominant mode of failure.

Using Equation (19), the plate reinforcement ratio for when compression rebars have yielded is calculated as:

$$\rho_{p,cy} = 0.0128.$$

Choosing a plate with nominal dimensions of: $t_p = 10$ mm, $b_p = 360$ mm, the plate reinforcement ratio is obtained as: $\rho_p = 0.0164$.

Since $\rho_p >$ larger of $\rho_{p,bb}$ and $\rho_{p,cy}$, Equation 14 is used to calculate the depth of the neutral axis, and subsequently Equation 13 is used to obtain the nominal flexural capacity:

$$c = 239 \text{ mm}$$

$$M_n = 1\,294 \text{ kN-m}$$

$$\phi M_n = 0.9 \times 1\,249 = 1\,164 \text{ kN-m.}$$

The above flexural capacity is very close to the required strength. Therefore, the plate is satisfactory from flexural point of view.

To check the local shear failure at the cut-off point, the properties of the strengthened section are calculated assuming uncracked section: $\bar{y} = 283$ mm, $I_{tr} = 9.75 \times 10^9$ mm⁴.

In calculating the maximum shear and normal stresses at the cut-off point, only that portion of the load which is applied after strengthening is considered, *i.e.*:

$$q = (120 - 75) \times 1.7 = 76.5 \text{ kN/m.}$$

Using the values for q , \bar{y} , I_{tr} and assuming $L_o = 100$ mm, Equation 20 results in: $\tau_{max} = 0.371$ MPa.

Parameters required for Equation 21 are calculated as: $K_n = 1\,029 \frac{\text{MPa}}{\text{mm}}$, $\beta = 0.095 \frac{1}{\text{mm}}$, $\gamma = 3.17$.

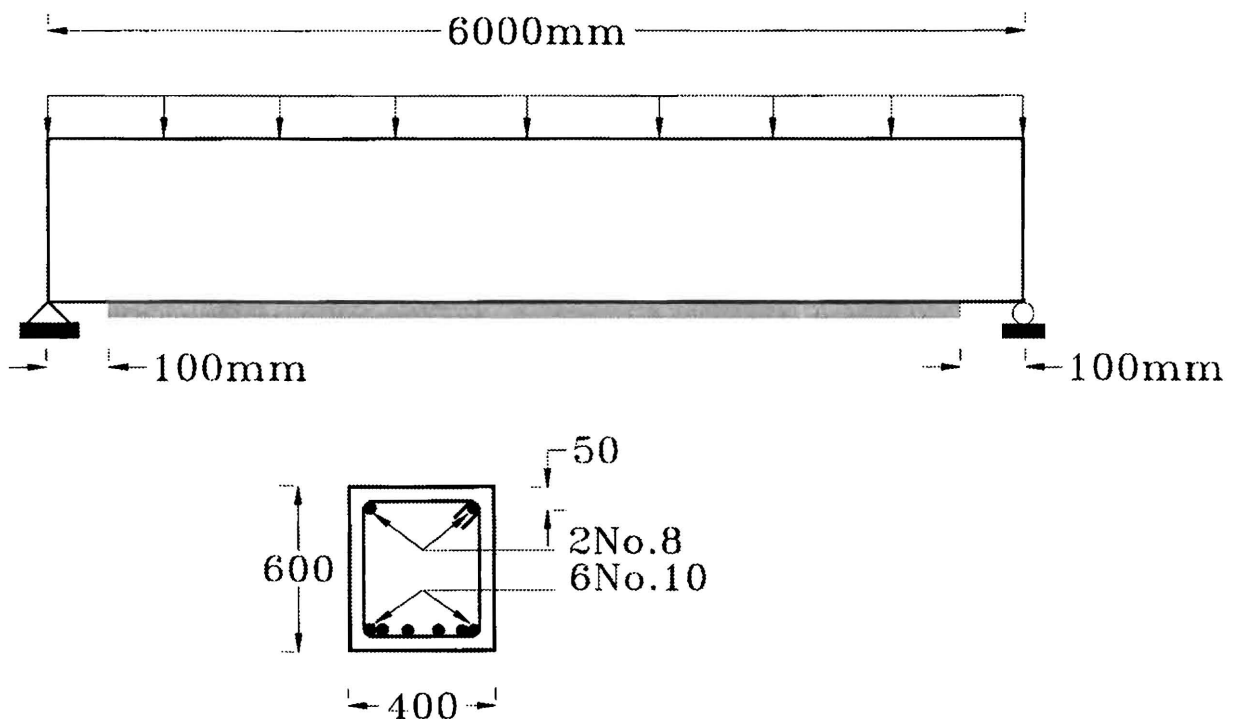


Figure 10. Details of Concrete Beam.

Consequently, the maximum peeling stress is calculated as: $f_{n,max} = 0.72$ MPa.

Using Equation 22, the increase in the bending moment is obtained as: $M_m = 4$ kN-m.

The bending moment in the concrete beam at the plate cut-off point due to factored loads before strengthening is calculated as 76.7 kN-m. Therefore, the total bending moment at the cut-off point is: $M = 80.7$ kN-m. The above moment is used to calculate the tensile stress in the concrete: $\sigma_x = 2.26$ MPa. Using stress transformation equations, the maximum principle stress is calculated as: $\sigma_1 = 2.35$ MPa.

Based on Equation 23, the ultimate capacity of concrete under biaxial state of stresses is 3.15 MPa, which is greater than the maximum principle stress. Therefore, the chosen plate provides adequate increase in the flexural capacity without local shear failure.

CONCLUSIONS

Fiber composite laminates can be bonded to tension face or web of reinforced concrete beams to increase stiffness and strength of the beam. The superior properties of composites, *i.e.*, corrosion-resistance, high strength, light weight, have made them attractive materials for this application. In experimental studies of reinforced concrete beams strengthened with composite laminates, the effect of the laminate has been reported to be significant in increasing the ultimate flexural and shear strengths.

Very few analytical studies, however, have been performed on this type of structure. Design guidelines and equations presented in this paper provide a basis for the design of this retrofitting system. The equations for shear and normal stress concentrations were verified with experimental results. Different modes of failure such as compression crushing of concrete, rupture of the plate, and local failure have been included in the design guidelines.

ACKNOWLEDGEMENT

The work presented in this paper was sponsored by the National Science Foundation under Grant No. MSS-9257344. The support of the National Science Foundation is greatly appreciated. The opinions, findings, and conclusions outlined in this paper are those of the authors and they do not represent the views of the National Science Foundation.

REFERENCES

- [1] M.D. MacDonald and A.J.J. Calder, "Bonded Steel Plating for Strengthening Concrete Structures", *International Journal of Adhesion and Adhesives*, **2**(2) (1982), pp. 119–127.
- [2] D.A. Van Gemert and M.C.J. Vanden Bosch, "Repair and Strengthening of Reinforced Concrete Structures by Means of Epoxy Bonded Steel Plates", *Proceedings of the International Conference on Deterioration, Bahrain*, 1985, pp. 181–192.
- [3] Y.N. Ziraba, M.H. Baluch, I.A. Basunbul, A.M. Sharif, A.K. Azad, and G.J. Al-Sulaimani, "Guidelines Toward the Design of Reinforced Concrete Beams with External plates", *ACI Structural Journal*, **91**(6) (1994), pp. 639–646.
- [4] A. Sharif, G.J. Al-Sulaimani, I.A. Basunbul, M.H. Baluch, and M. Husain, "Strengthening of Shear-Damaged RC Beams by External Bonding of Steel Plates", *Magazine of Concrete Research*, **47**(173) (1995), pp. 329–334.
- [5] M.H. Baluch, Y.N. Ziraba, A.K. Azad, A.M. Sharif, G.J. Al-Sulaimani, and I.A. Basunbul, "Shear Strength of Plated RC Beams", *Magazine of Concrete Research*, **47**(173) (1995), pp. 369–374.
- [6] A.M. Malek and H. Saadatmanesh, "Physical and Mechanical Properties of Typical Fibers and Resins", *Proceedings of the First International Conference on Composites in Infrastructure, Tucson, AZ, U.S.A.*, (1995), pp. 68–79.
- [7] H. Saadatmanesh and M.R. Ehsani, "RC Beams Strengthened with FRP Plates I: Experimental Study", *ASCE Journal of Structural Engineering*, **117**(11) (1995), pp. 3417–3433.
- [8] P.A. Ritchie, D.A. Thomas, L.-W. Lu, and G.M. Connelly, "External Reinforcement of Concrete Beams Using Fiber Reinforced Plastics", *ACI Structural Journal*, **88**(4) (1991), pp. 490–500.
- [9] W. An, "Strengthening of Concrete Beams With Composite Plastic Plates", *M.S. Thesis, Department of Civil Engineering and Engineering Mechanics, University of Arizona, Tucson, Arizona, U.S.A.*, 1990.
- [10] W. An, H. Saadatmanesh, and M.R. Ehsani, "RC Beams Strengthened with FRP Plates, II: Analysis and Parametric Study", *ASCE Journal of Structural Engineering*, **117**(11) (1991), pp. 3434–3455.
- [11] A.M. Malek, "Analytical Study of Reinforced Concrete Beams Strengthened with Fiber Reinforced Plastic Plates (Fabrics)", *Ph.D. Dissertation, Department of Civil Engineering and Engineering Mechanics, University of Arizona, Tucson, AZ, U.S.A.*, 1997.

- [12] A.M. Malek, H. Saadatmanesh, and M.R. Ehsani, "Prediction of Failure Load of Reinforced Concrete Beams Strengthened with FRP Plates Due to Stress Concentrations at the Plate End", *ACI Structural Journal*, **95**(2) (1998), pp. 142–152.
- [13] H. Saadatmanesh and A.M. Malek, "Design Guidelines for Flexural Strengthening of Reinforced Concrete Beams with FRP Plates", *ASCE Journal of Composites in Construction*, **2**(4) (1998), pp. 158–164.
- [14] T. Norris, H. Saadatmanesh, and M.R. Ehsani, "Shear and Flexural Strengthening of R/C Beams with Carbon Fiber Sheets", *ASCE Journal of Structural Engineering*, **123**(7) (1997), pp. 903–911.
- [15] A.M. Malek and H. Saadatmanesh, "Analytical Study of R/C Beams Strengthened with Web-Bonded FRP Plates or Fabrics", *ACI Structural Journal*, **95**(3) (1998), pp. 343–352.
- [16] A.M. Malek and H. Saadatmanesh, "Ultimate Shear Capacity of R/C Beams Strengthened with Web-Bonded FRP Plates or Fabrics", *ACI Structural Journal*, **95**(4) (1998), pp. 391–399.
- [17] H.B. Kupfer and K.H. Grestle, "Behavior of Concrete Under Biaxial Stresses", *ASCE Journal of the Engineering Mechanics Division*, **99**(EM4) (1973), pp. 853–866.

Invited Paper Received 11 February 1998.